J Mater Sci (2007) 42:5248–5255
DOI 10.1007/s10853-006-0389-9

Magnetic properties of nanocrystalline magnesium ferrite by co-precipitation assisted with ultrasound irradiation

Mohamed Mohamed Rashad

Received: 5 December 2005 / Accepted: 1 May 2006 / Published online: 31 January 2007

Abstract Magnesium ferrite $MgFe_2O_4$ nanopowders were synthesized using chemical co-precipitation assisted with ultrasound irradiation technique. The ferrite precursors were precipitated from the corresponding sulfates by 5 M sodium hydroxide at pH 11 without and with ultrasound irradiation for 2–6 h. Thermal treatment of the produced precursors with and without ultrasound irradiation for 2 h at temperature ranged from 600 to 1,000 °C was also studied. The powders formed were characterized by X-ray diffraction (XRD), Fourier transformer infrared (FT-IR), scanning electron microscope (SEM) and vibrating sample magnetometer (VSM). Effects of ultrasound irradiation time, calcination temperature and Fe/Mg mole ratio on the phase formation and magnetic properties were reported. Pure crystalline $MgFe_2O_4$ phase can be obtained by thermal treatment of the precursor at temperature 1,000 °C with ultrasound irradiation for 2 h with high magnetization (18.39 emu/g).

Introduction

Magnesium ferrite, $MgFe_2O_4$, is one of the important magnetic oxides with spinel structure. Apart from its magnetic application in the area of memory and switching circuits of digital computers and microwave devices, Mg ferrite is used as a catalyst in dehydrogenation of butene, humidity sensor and recently is more applicable in achieving local hyperthermia when compared with other ferrites [1–7]. There are several methods for synthesizing nanosized magnesium spinel ferrite particles, such as ceramic [8–10], co-precipitation [11], microwave hydrothermal method, [5], sol gel [12], citrate gel process [13], combustion method [14–16], high energy milling [17], and mechanical alloying [18]. Ultrasound irradiation has been routinely used in the field of materials science. It has proven to be a useful method for the preparation of novel materials [19, 20]. Many materials in literature are synthesized by ultrasound irradiation included MgO [21], CdS and CdSe [22–24], ZrO_2 [25], Co_3O_4 and NiO [26], PbS, PbSe and PbTe [27], $NiAl_2O_4$ [28], Cu–Ni ferrites [29], barium hexaferrite [30] and Mn–Zn ferrites [31] and etc.... The chemical effects of ultrasound irradiation arise from acoustic cavitation, that is the formation, growth and implosive collapse of the bubble in a liquid. The implosive collapse of the bubble generates localized hot spots and microjet impacts on the materials, which can result in activating reaction, particle size reduction, surface cleaning and so on. These hot spots have been shown to have a transient temperature of about 5,000 K, pressure of 188 atm., and cooling rates of 10^8 K/s [19]. In this study, we aim to synthesis of magnesium spinel ferrite nanopowders adopting co-precipitation with and without ultrasound irradiation. The changes in microstructure and magnetic properties of the spinel ferrite are investigated.

M. M. Rashad (✉)
Central Metallurgical Research and Development Institute (CMRDI), P.O. Box 87, Helwan, Cairo, Egypt
e-mail: rashad133@yahoo.com

Experimental

Mg spinel ferrite nanopowders were prepared using the co-precipitation and co-precipitation assisted by ultrasonic irradiation methods. The starting materials used ammonium ferrous sulfate $(NH_4)_2Fe(SO_4)_2 \cdot 6H_2O$ and magnesium sulfate heptahydrate $MgSO_4 \cdot 7H_2O$ were dissolved in bidistilled water and mixed together taking in our consideration the Fe/Mg mole ratio 2:1. The produced solution was treated with 5 M NaOH to form a precipitate at pH 11. The produced slurry was filtered, washed and dried at 100 °C. The formed precursor powders were calcined at 600–800 °C for 2 h in static air atmosphere. For using ultrasound irradiation (20 kHz, 750 W), the precipitated slurry formed at pH 11 was treated by ultrasound irradiation for time intervals from 2 to 6 h. The precipitated was filtered, washing, and then dried at 100 °C. The produced precursors powders using ultrasound irradiation for 2 h were calcined at temperature ranged from 600 to 1,000 °C. The X-ray diffraction (XRD) patterns of the resulting products were characterized by a Brucker D8-advance X-ray powder diffractometer with CuKα radiation (λ = 1.5406 Å) in the 2θ range from 10 to 80° with time per step 1.000 second and step size (2θ) 0.02. The micrograph of $MgFe_2O_4$ was examined by direct observation via scanning electron microscope (SEM) model (JSM-5400). The magnetic properties of the ferrites were characterized by a vibrating sample magnetometer (VSM; 9600-1 LDJ, USA). Vibration spectrum of the magnesium ferrite powder in KBr was recorded on Fourier Transformer and Pye-Unicam SP 300 instrument.

Results and discussion

X-ray diffraction patterns of precursors samples precipitated at pH 11 without and with ultrasound irradiation treated for time intervals from 2 to 6 h are shown in Fig. 1. The XRD patterns of the precursor without ultrasound irradiation treatment is magnesium ferrite with nearly amorphous impurities showing five spread peaks at 2θ values of 30.30°, 35.67°, 43.29°, 52.89°, 57.30° and 63.021° which ascribed to magnesium iron oxide $MgFe_2O_4$ phase (JCPDS Card # 73-1720). The diffraction peaks are corresponding to (220), (311), (400), (422), (511) and (440) planes. For ultrasound irradiation treated sample for 2 h, the diffraction peaks corresponding to (220), (311), (400), (422), (511) and (440) planes of polycrystalline $MgFe_2O_4$ phase are confirmed. By increasing the ultrasound irradiation time for 4 h, it is clear that the diffraction peaks are related to magnesium ferrite and muskoxite $Mg_{0.7}Fe_{0.4}O_{1.3} \cdot H_2O$ (JCPDS Card # 22-0709). Eight peaks related to 2θ values of 18.6°, 30.30°, 35.67°, 43.29°, 46.9°, 52.89°, 57.34° and 63.02° ascribed to magnesium ferrite. In addition, the peaks are related to muskoxite at 2θ values of 34.69°, 39.80°, 52.98° and 62.80°. Increasing the ultrasound irradiation time to 6 h, the formed phases are magnesium ferrite, muskoxite and weak crystalline peaks and low intensity of iron hydroxide (JCPDS Card # 22-0346). This is may be due to the dissociation of the produced magnesium ferrite powders by increasing ultrasound irradiation time up to 6 h. Other experiment is carried out by ageing the produced hydroxide slurry in water for 6 h. The results showed that the XRD of the produced precursor sample has not changed compared with the formed precursor powders directly from the hydroxide slurry.

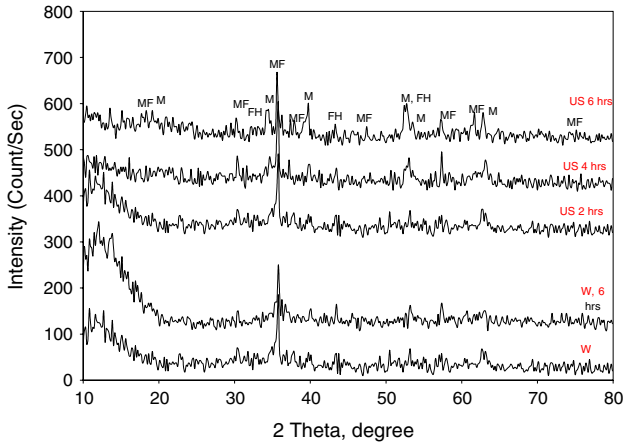

Fig. 1 XRD patterns of the produced magnesium ferrite powder without (W, W and 6 h) and with 2, 4 and 6 h ultrasound irradiation time (MF, magnesium ferrite; M, muskoxite; FH, iron hydroxide)

The crystallite size of $MgFe_2O_4$ for the most intense peak (311) plane determines from the X-ray diffraction data using the Debye–Scherrer formula:

$$d_{RX} = k\lambda/\beta\cos\theta$$

Where d_{RX} is the crystallite size, k = 0.9 is a correction factor to account for particle shapes, β is the full width at half maximum (FWHM) of the most intense diffraction peak (311) plane, λ is the wavelength of Cu target = 1.5406 Å, and θ is the Bragg angle. The average crystallite size of the precipitated precursor sample without ultrasound irradiation is 49.3 nm and for the sample ageing in water for 6 h is 49.7 nm. On the other hand, the average crystallite

sizes are 27.2–39.7 nm with ultrasound irradiation time from 2 to 6 h.

As the temperature changes, the crystallinity and purity of magnesium ferrite change. Figure 2 shows the XRD patterns of magnesium ferrite powders with and without ultrasound irradiation time for 2 h at thermal temperature from 600 to 1,000 °C for heating time 2 h. At 600 °C, the produced powders without ultrasound irradiation are nearly magnesium ferrite. Six crystalline intensity peaks are appeared at 2θ values of 30.30°, 35.67°, 43.29°, 52.89°, 57.34° and 63.02°, respectively. These peaks ascribed to (220), (311), (400), (422), (511) and (440) diffraction planes of $MgFe_2O_4$ phase. On the other hand, the XRD of the precursor sample with ultrasound irradiation time for 2 h and thermally treated at 600 °C showed six peaks of magnesium ferrite with high crystallinity compared with the sample without ultrasound irradiation. In addition, iron oxide peaks are also formed (JCPDS Card # 02-0915). Peaks related to iron oxide are appeared at 2θ values 33.13, 36.01 and 53.98°. The average crystallite size of the mean intense peak (311) is 27.2 and 38.0 nm with and without ultrasound irradiation for 2 h and thermally treated at 600 °C, respectively. As the temperature increases to 800 °C, the formed powders phases are magnesium ferrite and iron oxide for the sample without ultrasound treatment. Peaks related to iron oxide are formed at 2θ values of 24.16°, 33.18°, 43.15°, 49.90° and 64.05°. On the other hand, XRD patterns of the ultrasound irradiation sample for 2 h and thermally treated at 800 °C showed that $MgFe_2O_4$ phase with high crystalline intensity and weak peaks of iron oxide are formed. The mean crystallite sizes are 34.4 and 56.2 nm for ferrite samples produced at 800 °C with and without ultrasound irradiation for 2 h, respectively. As the temperature increases up to 1,000 °C, $MgFe_2O_4$ single phase is formed. The average crystallite sizes of the thermally treated precursors at 1,000 °C are 117.3 and 112 nm without and with ultrasound irradiation for 2 h, respectively.

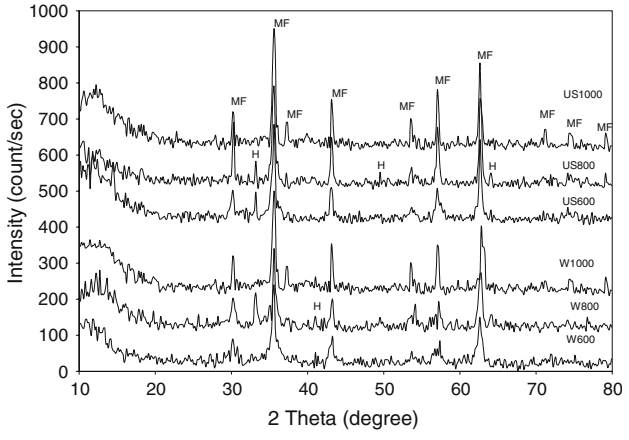

Fig. 2 XRD patterns of magnesium ferrite precursors calcined at different temperature from 600 to 1,000 °C without and with ultrasound irradiation for 2 h (MF, magnesium ferrite; H, iron oxide)

In order to investigate the influence of Fe/Mg mole ratio of phase identification and crystallization of ferrites powders, two precursors at Fe/Mg mole ratios 2:1 and 2:1.2 are prepared and thermally treated at 1,000 °C for 2 h. The XRD patterns of the produced powders samples are shown in Fig. 3. The results showed that the peaks attributed to $MgFe_2O_4$ phase are detected. The crystallization of magnesium ferrite is increased by increasing Fe/Mg mole ratio to 2:1.2. Samples obtained have homogeneous and uniform particle size. The average crystallite size was 112 and 117 nm, respectively. This is probably the reason for the highest magnetization obtained as will be shown later.

Scanning electron microscope photomicrographs of precursors samples without and with ultrasound irradiation for 2 h are shown in Figs. 4 and 5. The samples are uniform in shape and the crystallite size of two samples corresponded well to their X-ray diffraction calculation size. EDAX analysis of samples calcined at 1,000 °C without and with ultrasound irradiation for 2 h showed that chemical composition are oxygen 47.7%, Mg 9.70% and Fe 42.59% while in case ultrasound irradiation for 2 h, the constituents are oxygen 44.20%, Mg 8.47% and Fe 47.33%. The EDAX analyses showed that Fe/Mg mole ratios are nearly 2:1 and 2:0.82 with and without ultrasound irradiation for 2 h, respectively. This is due to dissolve of small part of magnesium hydroxide during ultrasound irradiation.

FT-IR spectrum of the powder precursors without and with 2, 4 and 6 h ultrasound irradiation times is

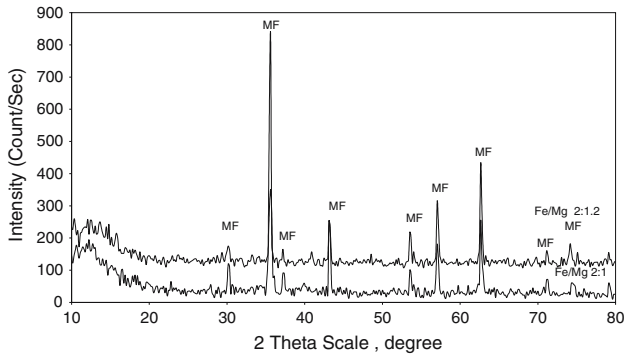

Fig. 3 XRD patterns of the magnesium ferrite powder produced at different Fe/Mg mole ratios

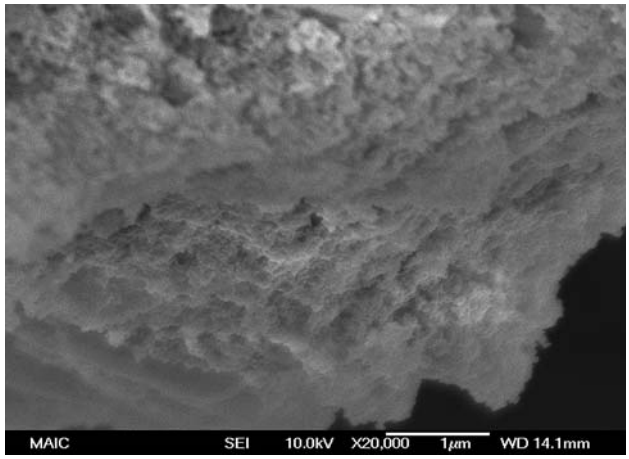

Fig. 4 SEM of the produced magnesium ferrite precursor powders produced without ultrasound irradiation time

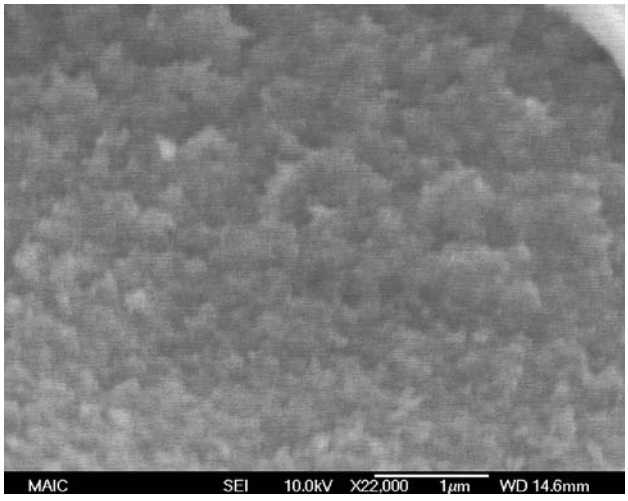

Fig. 5 SEM of the produced magnesium ferrite precursor powders produced with ultrasound irradiation for 2 h

showed in Fig. 6. Generally, the FT-IR spectrum of the precursors without and with 2 h ultrasound irradiation times for 2 h is nearly the same. The bands near 3,000–3,600 cm^{-1} assigned to the stretching vibrations of the hydrogen-bonded OH groups. Absorption bands due to the iron–oxygen bonds (corresponding to iron located in octahedral and tetrahedral bands), are observed in the 450–540 cm^{-1} and also the presence of α-Fe_2O_3. The presence of the band at 635 cm^{-1} is due to the molecular water. The bands produced at 1,635 cm^{-1} for all samples powders are due to the presence of H_2O. The other peaks formed are due to the presence of magnesium ferrite.

The magnetic properties of $MgFe_2O_4$ powders prepared with and without different ultrasound irradiation time is measured using vibrating sample magnetometer. Magnetization is performed at room temperature and hysteresis loops of the ferrite powders were obtained. Plots of magnetization (M) as a function of applied magnetic field (H) per time, temperature and Fe:Mg mole ratio were given in Figs. 7–9. The corresponding magnetization hysteresis curves for powders produced at without and with ultrasound irradiation time ranged from 2 to 6 h and pH 11 are shown in Fig. 7. Apparent superparamagnetic behavior is always observed for all samples at room temperature. Table 1 lists effect of ultrasound irradiation treatment time on the coercive force (Hc), saturation magnetization (Ms), remenant magnetization (Mr) and the ratio of remenant magnetization to saturation magnetization (Mr/Ms). It is clear that the magnetic properties are changed by changed the ultrasound irradiation time, Hc without ultrasound irradiation time is 45.89 Oe increases to 58.02 Oe at ultrasound irradiation for 2 h to 68.03 Oe at ultrasound

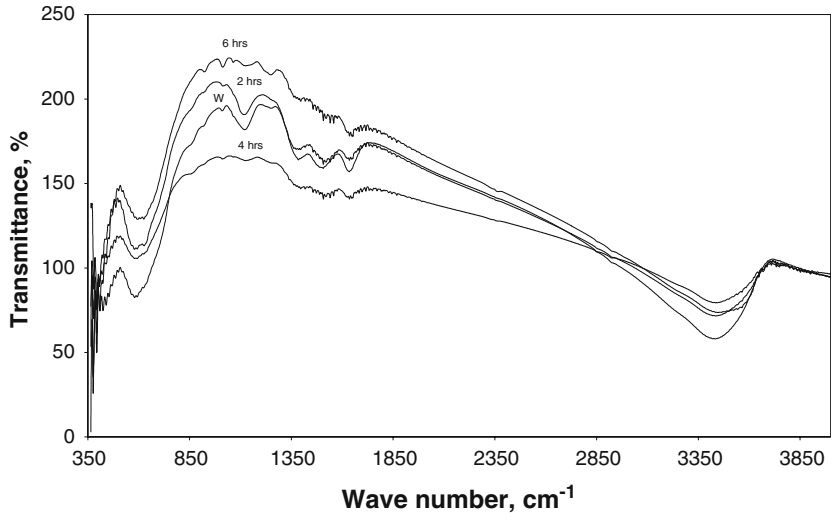

Fig. 6 FT-IR spectrum of the produced magnesium ferrite powders without and with 2, 4 and, 6 h ultrasound irradiation times

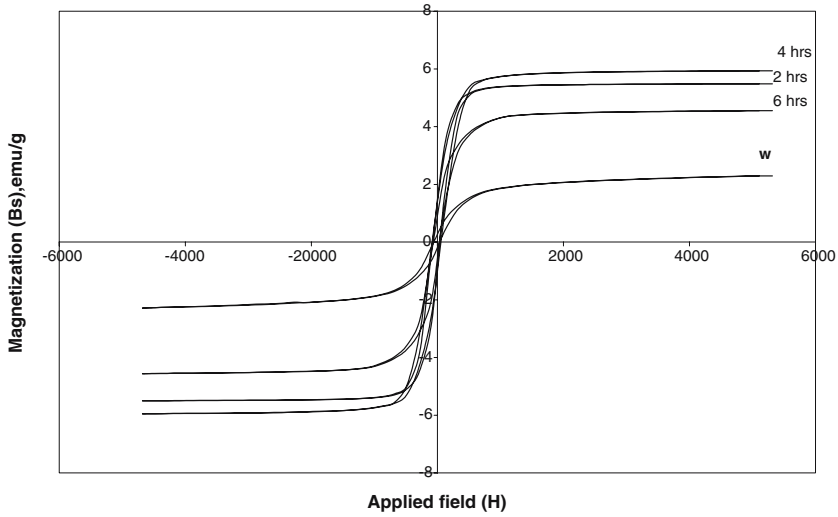

Fig. 7 The magnetization hysteresis of $MgFe_2O_4$ precursors powders prepared without and with 2, 4 and 6 h ultrasound irradiation

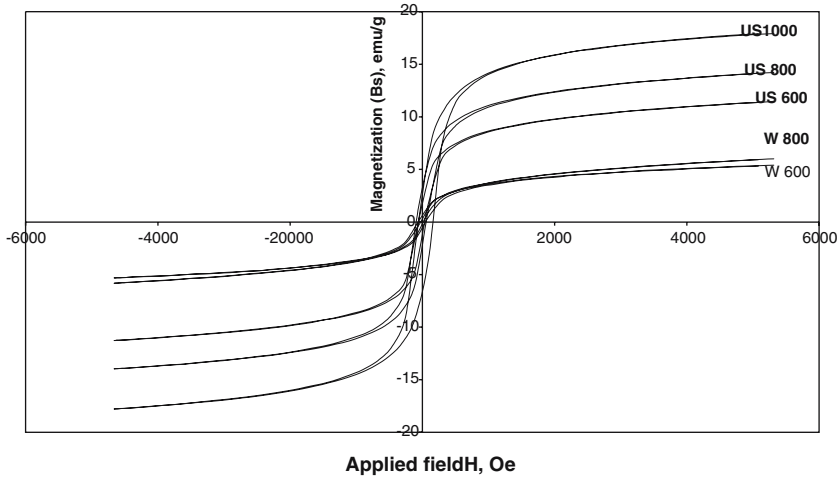

Fig. 8 The magnetization hysteresis of the produced magnesium ferrite powders calcined at different temperature with and without 2 h ultrasound irradiation

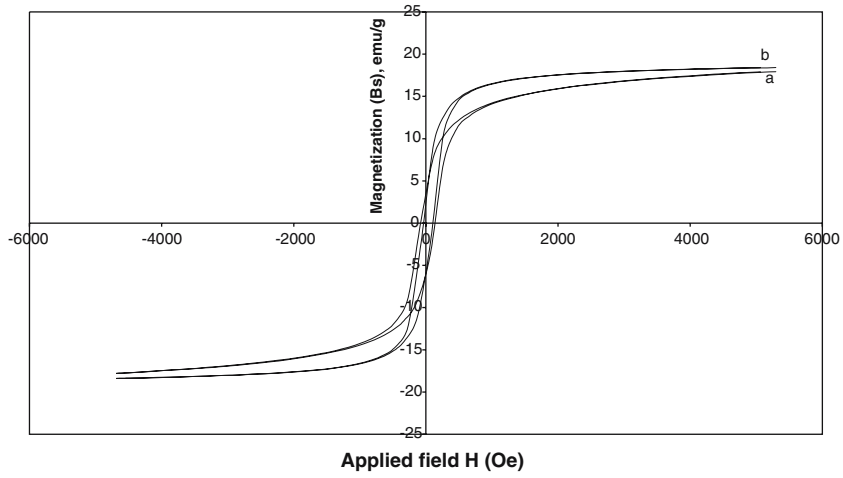

Fig. 9 Magnetization hysteresis of the produced magnesium ferrite powder produced from the precursor 2 h ultrasound irradiation time calcined at 1,000 °C for 2 h at (a) Fe/Mg mole ratio 2:1 (b) Fe/Mg mole ratio 2:1.2

irradiation time for 4 h and then the decrease changes observed at 6 h (50.14 Oe). The change of the value of coercive force may be due to the low crystalline anisotropy, which arises from crystal imperfection and the high degree of aggregation. In addition, the magnetic properties are dependent on the morphology

Table 1 Effect of time of ultrasound irradiation on the magnetic properties of the produced $MgFe_2O_4$ powders

Time	Ms (emu/g)	Mr (emu/g)	Hc (Oe)	Mr/Ms
W	2.291	0.188	45.89	0.082
2	5.494	0.842	58.02	0.153
4	5.946	0.909	68.03	0.153
6	4.558	0.602	50.14	0.132

W, sample without ultrasound irradiation

of the particles and the uniaxial microstructure of the final products. Remenant magnetization increases from 0.188 emu/g for the powder without ultrasound irradiation to 0.842 emu/g then increases to 0.909 emu/g and then decreases to 0.602 emu/g at 6 h. The saturation magnetization increases from 2.291 emu/g for the sample without ultrasound irradiation to 5.494 emu/g for the sample with ultrasound irradiation for 2 h to 5.946 emu/g at 4 h and then decreases to 4.558 emu/g for 6 h. The decrease in these values could result from the existence of spin canting, which has been reported, in several nanometer-sized ferrites [32] which is attributed to surface structure disorder. It is known that the energy of a magnetic particle in the external field is proportional to its size via the number of magnetic molecules in a single magnetic domain. When this energy becomes comparable to thermal energy, thermal fluctuations will significantly reduce the total magnetic moment at a given field. This is due to the large surface-to-volume ratio for ultrafine particles. The magnetic molecules on the surface lack the complete co-ordination and the spins are disordered. Another possible reason for the diminution in Ms may be the incomplete crystallization of $MgFe_2O_4$ particles, which lead to amorphous impurities undetectable by XRD, e.g., magnesium hydroxide and iron hydroxide are decreased the magnetic properties of the produced magnesium ferrite powders. Also, presence of non-magnetic materials like muskoxite and iron oxide decreased the magnetization of the formed ferrite powders. The low values of Mr/Ms ratio indicate an appreciable fraction of superparamagnetic particles. For the precipitated sample without ultrasound irradiation, Mr/Ms value is 0.082 without ultrasound irradiation then increases to 0.153 for ultrasound irradiation for 2 and 4 h then decreased to 0.132 at 6 h, which indicate that a fraction of the particles is in the blocked state.

Figure 8 shows the magnetic hysteresis of $MgFe_2O_4$ nanopowders prepared without and with ultrasound irradiation for 2 h and thermally treated at temperature ranged from 600 to 1,000 °C for 2 h. The magnetic properties are summarized in Table 2. The results

Table 2 Magnetic properties of the produced $MgFe_2O_4$ powders at different calcination temperature with and without 2 h ultrasound irradiation time

Time	Ms (emu/g)	Mr (emu/g)	Hc (Oe)	Mr/Ms
W600	5.909	0.366	19.79	0.062
W800	5.354	0.536	57.26	0.100
US600	11.37	1.282	48.86	0.113
US800	14.09	1.905	75.99	0.135
US1000	18.39	2.525	68.11	0.137

W600 and W800 precipitated samples at 600 and 800 °C without ultrasound irradiation US600, US800 and US1000, precipitated samples calcined at 600, 800 and 1,000 °C with 2 h ultrasound irradiation

showed that the magnetic properties are temperature dependent. Hc is increased from 19.79 to 57.26 Oe when the temperature increased from 600 to 800 °C for the powders produced without ultrasound irradiation. On the other hand, Hc is increased from 48.86 at 600 °C to 75.99 Oe at 800 °C and then decreased to 68.11 Oe at 1,000 °C, respectively for the powders produced with ultrasound irradiation time for 2 h. This may be attributed to the change in the crystallite size range from 34 to 112 nm. Mr shows a minimum value (0.062 emu/g) at 600 °C increased to 0.1000 emu/g at 800 °C for the ferrite powders produced without ultrasound irradiation. Also, Mr increased by increased the temperature from 0.113 to 0.137 emu/g when the thermal treated temperature increased from 600 to 1,000 °C for the magnesium ferrite powders produced with ultrasound irradiation for 2 h. The saturation magnetization (Ms) is increased slowly from 5.909 emu/g at 600 °C to 5.345 emu/g at 800 °C for the magnesium ferrite powders without ultrasound irradiation. In contrast, Ms is increased from 11.37 emu/g at 600 °C to 14.09 emu/g at 800 °C and then 18.39 emu/g at 1,000 °C for magnesium ferrite powders produced by ultrasound irradiation for 2 h. This type of behavior is entirely consistent with a model of crystal growth in such a way that the difference in the magnetic parameters is associated with the change in crystal size [33].

The effect of Fe/Mg mole ratio on the magnetic hysteresis for $MgFe_2O_4$ powders produced after ultrasound irradiation for 2 h and thermally treated at 1,000 °C is shown in Fig. 9 and the magnetic properties are listed in Table 3. It is clear that Hc is increased by increased Fe/Mg mole ratios from 68.11 to 106.7 Oe when Fe/Mg mole ratio increased from 2:1 to 2:1.2, respectively. Mr is increased from 2.525 to 2.896 emu/g by changed the Fe/Mg mole ratios. The Mr/Ms ratio values are 0.137 and 0.162 for Fe/Mg mole ratios 2:1 and 2:1.2, respectively Saturation magnetization shows

Table 3 Effect of Fe/Mg mole ratio on the magnetic properties of the produced $MgFe_2O_4$ powders after 2 h ultrasound irradiation

Fe/Mg mole ratio	Ms (emu/g)	Mr (emu/g)	Hc (Oe)	Mr/Ms
2:1	18.39	2.525	68.11	0.137
2:1.2	17.85	2.896	106.7	0.162

a maximum value of (18.39 emu/g) at Fe/Mg mole ratio 2:1 and decreases slightly to 17.85 emu/g at Fe/Mg mole ratio of 2:1.2. These values are lower than the bulk value for the magnetization of the magnesium ferrites produced by ceramic method at 1,100 °C for 48 h (26.7 emu/g) [34] and it is also lower than the close reported value (27.0 emu/g) [35]. Meng et al. [35] produced magnesium ferrite with saturation magnetization (30.9 emu/g) by calcination Mg–Fe(III) layered double hydroxide intercalated by hexacyanoferrate (III) ions at 1,100 °C for 48 h. Misra et al. [36] discussed the lower of saturation magnetization than their bulk counterparts in terms of the two—component nanoparticles system consisting of a spin glass like surface layer and ferrimagnetically aligned core spins. Pradhan et al [37] showed that the magnetic properties of magnesium spinel ferrite are strongly dependent on the cations distribution among tetrahedral (A) and octahedral (B) sites in the cubic type-spinel structure where the structure formula of Mg-ferrite is usually written as $(Mg_{1-x}Fe_x)[MgFe_{2-x}]O_4$, where x represents the degree of inversion (defined as the fraction of (A) sites occupied by Fe^{3+} cations). In pure $MgFe_2O_4$, The Mg^{2+} ions are randomly distributed. Some Mg^{2+} ions will be forced to the A sites leading initially to the transfer of some Fe^{3+} ions from A to B site. This will give rise to an increased B site magnetization and then the magnetic interaction and magnetization steadily decrease due to the reduction in the Fe^{3+}.

Conclusion

Magnesium ferrite nanopowders are prepared using co-precipitation and co-precipitation assisted with ultrasound irradiation methods. Effects of ultrasound irradiation time and calcination temperature (600–1,000 °C) on the phase formation and magnetic properties of the produced magnesium ferrite powder are studied. The formed precipitated powders without ultrasound irradiation are mainly magnesium ferrite. Increasing ultrasound irradiation time up to 6 h decreases the magnesium ferrite phase. The average crystallite sizes are 49.3 and 27.2 nm without and with ultrasound irradiation time for 2 h. A well crystalline $MgFe_2O_4$ phase is obtained for the precursor treated with ultrasound irradiation for 2 h and thermally treated at 1,000 °C. The produced ferrites powders have superparamagnetic properties. The saturation magnetic magnetization (Ms), remenant magnetization (Mr) and coercive field (Hc) are 2.291 emu/g, 0.188 emu/g and 45.89 Oe without ultrasound irradiation, and 5.494 emu/g, 0.842 emu/g and 58.02 Oe with ultrasound irradiation for 2 h, respectively. The magnetic properties are enhanced by thermally treated precursor powder produced at ultrasound irradiation time for 2 h at different temperatures from 600 to 1,000 °C. The saturation magnetization (Ms), remenant magnetization (Mr) and coercive field (Hc) are enhanced to 18.39 emu/g, 2.525 emu/g and 68.11 Oe, respectively, for the ferrite powder produced at 1,000 °C, respectively.

References

1. Usca G, Finocchio E, Lorenzeli V, Trombetta M, Rossini SA (1996) J Chem Soc Faraday Trans 92:4687
2. Shimizu Y, Arai H, Seiyama T (1985) Sensor Actuator 7:11
3. Gusmano G, Montesperelli G, Morten B, Prudenziati M, Pumo A, Traversa E (1996) J Mater Process Technol 56(1–4):589
4. Maehera T, Konishi K, Kamimori T, Aono H, Naohara T, Kikkawa H, Watanable Y, Kawachi K (2002) Jpn J Appl Phys 41:1620
5. Verma S, Joy PA, Khollam YB, Potdar HS, Deshpande SB (2004) Mater Lett 1092
6. Paik JG, Lee M-J, Hyun S-H (2005) Thermochim Acta 425:131
7. Yang BL, Cheng DS, Lee SB (1991) Appl Catal 70:161
8. Kullarni RG, Joshi HH (1986) J Solid State Chem 64(2):141
9. Lakshman A, Rao KH, Mendiratta RG (2002) J Magn Magn Mater 250:92
10. Chhaya SD, Pandya MP, Chhantbar MC, Modi KB, Baldha GJ, Joshi HH (2004) J Alloys Comp 377:155
11. Chen Q, Rondinone AJ, Chakoumakos BC, Zhang ZJ (1999) J Magn Magn Mater 194:1
12. Oliver SA, Willey RJ, Hamdeh HH, Oliveri G, Busca G (1995) Scripta Metal Mater 33(10/11):1695
13. Berchmans LJ, Selvan RK, Kumar PNS, Augustin CO (2004) J Magn Magn Mater 279:103
14. Basahel SN, El-Bellihi AA, Gabal M, Diefallah El-HM (1995) Thermochim Acta 256(2):339
15. Patil KC, Gajapathy D, Pai Verneker VR (1982) Mater Res Bull 17:29
16. Rupard RG, Gallagher PK (1996) Thermochim Acta 272:11
17. Sepelak V, Baabe D, Mienert D, Litterst FJ, Becker KD (2003) Scripta Mater 48:91
18. Moustafa SF, Morsi MB (1998) Mater Lett 34:241
19. Suslick KS (ed) (1988) Ultrasound: its chemical, physical and biological effects. VCH, Weinheim
20. Suslick KS, Choe SB (1991) Nature 353:414
21. Stengl V, Bakardjieva S, Marikova M, Bezdicka P, Subrt J (2003) Mater Lett 57:3998
22. Li H-L, Zhu Y-C, Chen S-G, Palchik O, Xiong J-P, Koltypin Y, Gofer Y, Gedanken A (2003) J Solid State Chem 172:102

23. Zhou SM, Feng YS, Zhang LD (2003) Mater Lett 57:2936
24. Singh VP, Singh RS, Thompson GW, Jayaraman V, Samagapalli S, Rangrai VK (2004) Solar Energy Mater Solar Cells 81:293
25. Liang J, Jiang X, Liu G, Deng Z, Zhung J, Li F, Li Y (2003) Mater Res Bull 38:161
26. Srivastava DN, Perkas N, Seisenbaeva GA, Koltypin Y, Kessler VG, Gedanken A (2003) Ultrason Sonochem 10:1
27. Li Q, Ding Y, Shao M, Wu J, Yu G, Qian Y (2003) Mater Res Bull 38:539
28. Jeevanandam P, Koltypin Y, Gedanken A (2002) Mater Sci Eng B 90:125
29. Doh SG, Kim EB, Lee BH, Oh JH (2004) J Magn Magn Mater 272–276:2238
30. Shafi KVPM, Gedanken A (1999) Nanostruct Mater 12:29
31. Rao SS, Reddy CS, Ravinder D, Reddy BR, Reddy DL (2002) Mater Lett 56(3):175
32. Berkowitz E, Scuele WJ, Flanders PJ (1969) J Appl Phys 39(2):1261
33. Gregg SY, Sing KSW (1982) Pure Appl Chem 54:2210
34. Kulkani RG, Joshi HH (1986) J Solid State Chem 64:141
35. Meng W, Li F, Evans DG, Duan X (2004) Mater Chem Phys 86:1
36. Misra RDK, Gubbala S, Kale A, Egelhoff WF Jr (2004) Mater Sci Eng B 111:164
37. Pradhan SK, Bid S, Gateshki M, Petkov V (2005) Mater Chem Phys 93:224